Original Article

Tumor Biology

Tumor Biology
April 2017: 1–12

DOI: 10.1177/1010428317695033
journals.sagepub.com/home/tub
SAGE

The apoptotic and genomic studies on A549 cell line induced by silver nitrate

Ayse Kaplan[1], Gulsen Akalin Ciftci[2] and Hatice Mehtap Kutlu[1]

Abstract

Lung cancer is the leading cause of male cancer deaths worldwide. Metal-based anticancer drugs have evolved significantly during the past decades. Recently, silver ions have been investigated for their anticancer effects. We aimed to study the time-course cytotoxic effects of silver nitrate on A549 adenocarcinomic human alveolar basal epithelial cells to provide insights into the molecular-level understanding of growth suppression mechanism involved in apoptosis. The influences of silver nitrate were studied via MTT assay, flow cytometry, immunocytochemical, confocal and transmission electron microscopy, and microarray assays. Silver nitrate showed inhibitory effects against A549 cells in a dose- and time-dependent manner for 24, 48, and 72 h and induced apoptosis. The early and late apoptotic cells and depolarized mitochondrial membrane potential were determined by the half-maximal inhibitory concentration (IC_{50}) value of silver nitrate treated for 72 h. But cysteinyl aspartate proteinase-3 was not activated for 72 h. Furthermore, IC_{50} value of silver nitrate also induced apoptosis according to immunocytochemical assays for 72 h. The downregulated *CCNY*, *HNRNPL*, *ASF1B*, *PIAS4*, *HNRNPH1*, *EIF2C2*, *TAF15*, *FOXC1*, *LEP*, and *PCB2* genes administered with silver nitrate IC_{50} were identified as apoptosis-leading genes. Silver nitrate may be a suitable therapeutic agent against lung cancer.

Keywords

Silver nitrate, A549, apoptosis, flow cytometry, immunocytochemistry, microarray

Date received: 15 July 2016; accepted: 23 December 2016

Introduction

Lung cancer is one of the most widespread cancers and cause of death all around the world,[1–4] and most of the deaths are seen among men. Lung cancer includes mostly carcinomas,[1] and 31% of lung cancers are adenocarcinomas.[4] The A549 cells are adenocarcinomic human alveolar basal epithelial cells. The A549 cell line was first developed in 1972 by Giard et al.[5]

Silver compounds, especially silver nitrate, have been used in antimicrobial therapy over the last 20 years.[6,7] The anticancer potential of silver ions has gained significance in recent times.[8] Silver metal compounds are effective at low doses and high doses of silver nitrate have shown no renal toxicity in experimental animals (mouse).[9] Apoptosis or "programmed cell death" causes death of 50–70 billion cells every day in the average human adult. This process is called homeostasis and takes place for self-renewal of tissues, such as skin, gut, and bone marrow. The disruption of homeostasis can lead to cancer; and therefore, apoptotic genes have been focused at cancer treatment.[10,11]

The aim of this study was to determine the apoptotic signaling pathways that underlie the anticancer influences of silver nitrate on A549 adenocarcinomic human alveolar basal epithelial cells. We evaluated primarily the cytotoxicity of silver nitrate against A549 cells by the MTT (3-(4,5-dimethyl-2-thiazoyl)-2,5-diphenyl-2H-tetrazolium bromide) assay. Then, the effects on apoptosis were investigated using Annexin-V FITC/PI, cysteinyl aspartate proteinase (caspase)-3 labeling, mitochondrial membrane potential assay (JC-1 (5,5′,6,6′-tetrachloro1,1′,3,3′-tetramethylbenzimidazolylcarbocyanine iodide) labeling),

[1]Faculty of Science, Department of Biology, Anadolu University, Eskişehir, Turkey
[2]Faculty of Pharmacy, Department of Biochemistry, Anadolu University, Eskişehir, Turkey

Corresponding author:
Ayse Kaplan, Department of Biology, Faculty of Science, Anadolu University, 26470 Eskişehir, Turkey.
Email: aysekaplan26@hotmail.com

immunocytochemical assays, confocal microscopy, transmission electron microscopy, and microarray assay.

Materials

The A549 cells were purchased from American Type Culture Collection (ATCC, USA). Silver nitrate ($AgNO_3$) was purchased from HiMedia (India). Cisplatin and Roswell Park Memorial Institute (RPMI 1640) medium were from Sigma-Aldrich (USA), fetal bovine serum (FBS) and penicillin–streptomycin were from Gibco (South America, USA), Dulbecco's phosphate-buffered saline concentrate (10×) was from Biological Industries (Israel), trypsin/ethylenediaminetetraacetic acid (EDTA) solution was from Biochrom (Germany), MTT was from Alfa Aesar (Germany), and dimethylsulfoxide (DMSO) was from Sigma-Aldrich. The Annexin-V FITC/propidium iodide (PI) apoptosis detection kit, caspase-3 kit, and JC-1 kit were purchased from BD Biosciences (USA). The Annexin-V FITC, acridine orange, terminal deoxynucleotidyl transferase dUTP nick end labeling (TUNEL), bromodeoxyuridine (BrdU), hematoxylin/eosine, and Bcl-2 and Bax kits were purchased from Santa Cruz Biotechnology (USA). High pure RNA isolation kit (50 reactions) was obtained from Roche (Switzerland). Ambion total RNA Prep Kit (24 reactions) and HumanHT-12 v4 Bead Microarray Chip kit (12 reactions) were purchased from Illumina (USA).

Methods

Model cell line

The A549 cells were maintained in 75 cm^2 sterile plastic tissue culture flasks in RPMI medium supplemented with 10% (v/v) FBS and 1% penicillin/streptomycin (100 units/mL) as adherent monolayers. These cells were grown at 37°C in a humidified atmosphere containing 5% CO_2 in air.

Cell viability analysis

The A549 cells were cultured at a density of 5×10^3 cells per well in flat bottomed 96-well plates with various concentrations (1, 5, 10, 25, 50, 100, 125, 250, 500, and 1000 µM) of silver nitrate and cisplatin for 24, 48, and 72 h at 37°C in a humidified atmosphere containing 5% CO_2 in air. The main stock solution of the compound was prepared by dissolving in 0.1% DMSO and diluting in culture medium. After incubation, MTT powder (5 mg/mL) dissolved in phosphate-buffered saline (PBS) was added in each well (20 µL) for 2–4 h. Then, the medium was removed from the plate and 100 µL of DMSO was added in each well to dissolve the dye and kept for 10 min. The cells were measured at 540 nm using microtiter plate reader (BioTek Instruments ELx808IU, USA). Cell viability was calculated as a percent ratio and compared with the control cells. Each concentration was repeated in three wells and half-maximal inhibitory concentration 50 (IC_{50}) values were defined as the drug concentrations that reduced absorbance to 50% of control values. Three independent experiments were conducted to arrive at this IC_{50} value.

The determination of early/late apoptosis by flow cytometry

The A549 cells were seeded at 10^5 cells/mL per well in six-well plates at 37°C in a humidified atmosphere containing 5% CO_2 in air. Then, cells were treated with silver nitrate (13.5 µM) and cisplatin (3 µM) at IC_{50} doses for 72 h. The A549 cells were harvested and washed twice with ice-cold PBS and resuspended in 100 µL of binding buffer. A volume of 5 µL (5 µg/mL) of Annexin V-FITC and PI were added to the A549 cells and incubated for 15 min in the dark at room temperature (20–25°C). Then, 400 µL of binding buffer was added to the mixture samples and analyzed with a flow cytometer (BD FACS Aria Cell Sorter flow cytometry, BD Biosciences).

The analysis of caspase-3 by flow cytometry

The A549 cells were plated at a density of 10^5 cells in six-well plates at 37°C in a humidified atmosphere containing 5% CO_2 in air, and treated with IC_{50} doses of cisplatin (3 µM) and silver nitrate (13.5 µM) for 72 h. After treatment, the cells were harvested and washed twice with PBS. Then, the cells were suspended in BD Cytofix/Cytoperm (0.5 mL for each sample, BD Biosciences) and incubated for 20 min on ice. After incubation, the cells were centrifuged and the supernatant was discarded. Then, each of the samples was washed twice with 1× BD Perm/Wash buffer (0.5 mL for each sample, BD Biosciences). A volume of 100 µL of 1× BD Perm/Wash buffer and 20 µL of caspase-3 antibody were added to each sample and incubated for 30 min at room temperature. After incubation, the samples were washed with 1 mL BD Perm/Wash buffer and centrifuged. After centrifugation, the cells were suspended in 0.5 mL 1× BD Perm/Wash buffer and analyzed with a flow cytometer (BD FACS Aria Cell Sorter flow cytometry, BD Biosciences).

Analysis of mitochondrial membrane potential by flow cytometry

After being administered with IC_{50} doses of cisplatin (3 µM) and silver nitrate (13.5 µM) for 72 h in six-well plates, A549 cells were harvested and washed twice with PBS. The cells were centrifuged at 400*g* for 5 min and the supernatant was discarded. JC-1 dye solution (0.5 mL, 1× assay buffer + JC-1 stock solution) was added to each sample and incubated for 10–15 min at 37°C. After incubation, the cells were washed with 2 mL of 1× assay buffer and 1 mL of 1× assay buffer. Then, each of the samples were

suspended in 0.5 mL of 1× assay buffer and analyzed with a flow cytometer (BD FACS Aria Cell Sorter flow cytometry, BD Biosciences).

Immunocytochemical analysis

Fixation, paraffin embedding, and deparaffinization. The A549 cells were maintained in 75 cm^2 sterile flasks and administered with IC_{50} doses of cisplatin (3 μM) and silver nitrate (13.5 μM) for 72 h. Then, the cells were fixed overnight with 10% neutral-buffered formalin (900 mL distilled water (pH 7), 4 g sodium phosphate monobasic, 6.5 g sodium phosphate dibasic, and 100 mL of pure formaldehyde, (37%–40%)). Then, a little of paraffin was poured for paraffin embedding in the metal mold and the cells were placed in the mold. Then, the adhesion of cells was equally provided pressing on the base in cold. The cassette block was placed on the mold and the paraffin was added until it passed through the hole of the cassette block. The cassette block was then inserted into the holder slot. The tissue was trimmed to obtain integrity. Thin sections of, approximately, 4 μm were cut (ultramicrotome LEICA EM UC6, Leica Microsystems, Germany) and kept in the water bath at 45°C without shrinking. Then, the sections were transferred onto coverslides and sequentially to 60%, 70%, 80%, 90%, and 96% alcohol and incubated for about 1 h. Again, the sections were incubated in absolute alcohol. After incubation, acetone and xylene were added to the sections and incubated for 30 min. Deparaffinization lasted for 16 h, wherein the sections were incubated at 60°C for 1 h. After incubation, xylene was added three times to the sections for every 5 min. The sections were incubated in absolute alcohol and hydrated sequentially to 96%, 90%, 80%, 70%, and 50% alcohol for 1 min. The sections were then incubated in distilled water for 1 min and followed by staining procedure with hematoxylin.

Immunocytochemical staining

Hematoxylin and eosin staining. After incubating the sections in distilled water for 1 min, they were stained with hematoxylin, which was allowed to stand for 2 min. Again, the sections were incubated in distilled water for 1 min. A volume of 0.3% acid alcohol was added to remove overstaining. Then, the sections were incubated in distilled water for 1 min. Ammonia water (1%) was added to the sections, and the sections were immersed in 96% alcohol five times. Then, the sections were incubated with eosin Y (alcoholic) for 2 min and dehydrated in 70%, 90%, 96%, and absolute alcohol. Entellan was dropped on slides and 24 × 60 lamella was closed at 45°. The samples were then scanned by light microscopy.

TUNEL staining. The sections were washed with distilled water and exposed to Proteinase K enyzme at 37°C for 15 min. Then, they were washed with PBS and incubated with hydrogen peroxide (3% aqueous), PBS, and equilibration buffer for 3 min. The sections were then incubated with terminal deoxynucleotidyl transferase (TdT) enzyme working solution for 1 h, digoxigenin peroxidase secondary antibody for 30 min, and DAB (3,3′-diaminobenzidine) chromogen for 5 min. After incubation, acetone and xylene were added to the sections and kept for 30 min. The sections were incubated three times with paraffin for 30 min. Overall, the treatments lasted for 16 h. The samples were dehydrated in 70%, 90%, 96%, and absolute alcohol. Entellan was dropped on slides and 24 × 60 lamella was closed at 45°. The samples were then scanned by light microscopy.

BrdU labeling. An antigen retrieval step was applied to remove the masking antigen. The diluted citrate (pH 6, 1/10) was added to the sections. The sections were incubated in distilled water for 30 s. Then, the samples were incubated with PBS for 3 min, serum block solution for 5 min, and the primary antibody (BrdU) for 1 h. After incubation, the sections were washed with PBS for 3 min and the secondary antibody horseradish peroxidase (HRP) polymer was added and incubated for 20 min. Then, the samples were again washed with PBS for 3 min and incubated with DAB chromogen for 3 min. The samples were dehydrated in 70%, 90%, 96%, and absolute alcohol. Entellan was dropped on slides and 24 × 60 lamella was closed at 45°. The samples were then scanned by light microscopy.

Bcl-2 and Bax labeling. An antigen retrieval step was applied to remove the masking antigen. The diluted EDTA (pH 8, 1/10) was added to the sections. The sections were incubated in distilled water for 30 s and hydrogen peroxide (3% aqueous) for 10 min. Then, the samples were incubated with PBS for 3 min, serum block solution for 5 min, and the primary antibody (Bcl-2 and Bax) for 1 h. After incubation, the sections were washed with PBS for 3 min and incubated with the amplifier for 20 min. Then, the samples were again washed with PBS for 3 min. After washing, the samples were incubated with HRP polymer for 20 min, PBS for 3 min, aminoethyl carbazole (AEC) chromogen for 3 min, and washed with distilled water for 30 s. The samples were dehydrated in 70%, 90%, 96%, and absolute alcohol. Entellan was dropped on the slides and 24 × 60 lamella was closed at 45°. The samples were then scanned by light microscopy.

The evaluation via confocal microscopy

The A549 cells were plated onto sterilized coverslips in six-well plates, and exposed to the IC_{50} doses of cisplatin (3 μM) and silver nitrate (13.5 μM) for 72 h at 37°C. After exposure, the control and treated cells were washed with PBS and stained with Annexin-V FITC and acridine orange fluorescent dyes. Then, the structure of the cell membrane

and nucleus were observed, and structural changes were detected. The morphology was scanned by Leica TCS-SP5 II confocal microscopy and Leica Confocal Software version 2.00 was used for further analysis (Wetzlar, Germany).

Transmission electron microscopy

The A549 cells were grown in a 75 cm^2 sterile plastic tissue culture flask. The A549 cells with 80%–90% confluence were exposed to IC_{50} doses of cisplatin (3 μM) and silver nitrate (13.5 μM) for 72 h. Both the untreated and treated cells were incubated for 72 h. The effects of cisplatin and silver nitrate on A549 cells were determined using a transmission electron microscope (TEM, FEI Technai Biotwin, Hillsboro, Oregon, USA). The A549 cells were grown in Dulbecco's Modified Eagle's Medium (DMEM) medium and were fixed with 2.5% glutaraldehyde in 0.1 M PBS (pH 7.4) for overnight incubation at 4°C. After being embedded in agar and post fixation in 2% osmium tetroxide, cells were dehydrated in graded ethanol: 70, 90, 96, and 100%. The cells were then embedded in Epon 812 epoxy and sectioned with ultramicrotome (LEICA UC6, Wetzlar, Germany)).

Microarray analysis

The A549 cells were maintained at a density of 10^6–10^7 in 75 cm^2 plates at 37°C in humidified atmosphere containing 5% CO_2 in air. IC_{50} doses of cisplatin (3 μM) and silver nitrate (13.5 μM) were administered to the cells. Then, the cells were harvested and centrifuged. The supernatant was discarded. A volume of 200 μL of PBS was added to each sample pellet, and the samples were transferred to 2 mL Eppendorf tubes and stored at −80°C. Then, 400 μL of lysis/binding buffer was added to the samples and vortexed for RNA isolation. After centrifugation, 90 μL of DNase I incubation buffer + 10 μL of DNase I were added to the samples and incubated at room temperature for 15 min. After incubation, 500 μL of Wash Buffer I and Wash Buffer II were added and centrifuged at 8000*g* for 15 s. A volume of 2 μL of total messenger RNA (mRNA) + 1 μL of T7-Oligo(dT) primer were transferred to 200 μL polymerase chain reaction (PCR) tubes and incubated at 65°C for 5 min in a thermal cycler. After incubation, the samples were centrifuged and 2 μL of prepared mix (1.5 μL of v1-st-Strand cDNA PreMix + 0.25 μL of dithiothreitol (DTT) + 0.25 μL of SuperScript III Reverse Transcriptase = 2 μL of total reaction volume) was added to the samples and incubated at 50°C for 30 min in a thermal cycler. The strand DNA polymerase was incubated at 65°C for 10 min and spinned. Then, the samples were incubated at 80°C for 3 min and complementary DNA (cDNA) was obtained. Then, 2 μL of T7 transcription buffer + 3 μL of uridine triphosphate (UTP)/biotin-UTP + 10 μL of NTP PreMix + 3 μL of DTT + 2 μL of T7 RNA polymerase = 20 μL of total reaction volume was added to the samples for cDNA transcription at 42°C for 4 h. For complementary RNA (cRNA) synthesis, 20 μL of DNase-/RNase-free water and 100 μL of RNA binding buffer were added to the samples. Equivalent amount of ethanol was added to the mixture. The samples were then transferred to the column tube and were centrifuged at 12000*g* for 1 min. Then, 800 μL of RNA Wash Buffer was added and centrifuged at 12000*g* for 30 s. Again, the samples were washed with 400 μL of RNA Wash Buffer and centrifuged. The filter tube was removed from the collection tube to discard the supernatant and combined with the collection tube again to centrifuge the samples at 12000*g* for 2 min. A volume of 25 μL of DNase-/RNase-free water was added to each sample for the RNA transition in the column tube. In the next step, cRNA was diluted at hybridization in 200 μL tubes. The samples were incubated at 65°C for 5 min. Then, 5 μL of sample and 10 μL of hybridization buffer mixtures were transferred to 12 tubes. A volume of 200 μL of hybridization buffer was added to the slots on the chip platform. The chip was incubated in the hybridization oven at 58°C for 14–20 h. After hybridization, the chip was incubated in a water bath at 55°C. Then, the chip was dried at 1400 r/min for 4 min. Finally, the samples were scanned using Illumina Scan Control Software program of Illumina iScan (San Diego, California, USA).

Results

The cytotoxicity of silver nitrate on A549 cells

The cytotoxicity assays and determination of IC_{50} doses of cisplatin and silver nitrate in A549 human lung cancer cells were performed by MTT assay. The formazan formation was quantified spectrophotometrically at 540 nm using a microplate reader. The cytotoxic influences of cisplatin and silver nitrate were analyzed using 1, 5, 10, 25, 50, 100, 125, 250, 500, and 1000 μM doses for 24, 48, and 72 h, respectively (Figure 1). The antiproliferative and cytotoxic effects of cisplatin (Figure 1(a)) and silver nitrate (Figure 1(b)) were demonstrated as dose- and time-dependent reduction compared to control cells. The reduction on cell viability was observed in >90% of cells at 1000 μM dose. The IC_{50} doses of the substances were statistically calculated using Microsoft Excel 2010 (Redmond, Washington, USA) and 11.5 SPSS program (SPSS Inc., USA) (Table 1). IC_{50} of silver nitrate showed more cytotoxic effect than cisplatin for 24 h but cisplatin was more effective for 48 and 72 h (Table 1).

Effects of silver nitrate on early/late apoptosis

A549-treated cells were analyzed using fluorescence-activated cell sorting (FACS) in order to distinguish between early/late apoptotic and necrotic features. The IC_{50} of silver nitrate and cisplatin were administered to A549 cells for 72 h with each sample divided into two aliquots for

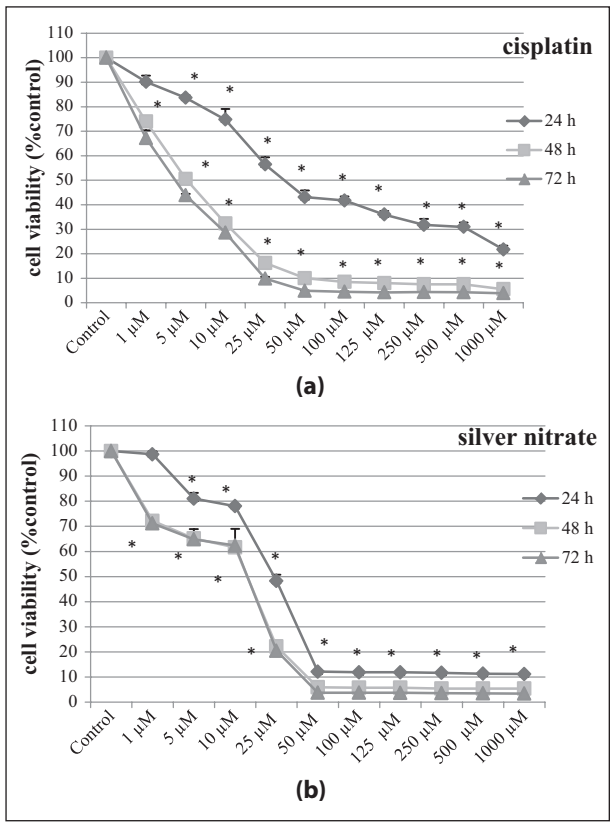

Figure 1. The cytotoxic and antiproliferative activities of silver nitrate and cisplatin against A549 adenocarcinomic human alveolar basal epithelial cells. The dose- and time-dependent effects were analyzed by MTT assay and the percentage viability was calculated: (a) cells treated with cisplatin; (b) cells treated with silver nitrate (data recorded as mean ± SD).
*$p < 0.05$ significantly different from control.

FACS analysis. One aliquot was stained with PI with degraded DNA to assess apoptotic cells. The second aliquot was used to evaluate the ruptured membranes of necrotic cells. Ruptured membranes of necrotic cells allow free PI uptake. PI is negative in early apoptotic and live cells but positive in late apoptotic cells (Figure 2). The late apoptotic cells increased 2.8-fold in cells administered with cisplatin (IC_{50} value; Figure 2(b); Table 2), and it was increased 1.7-fold in cells administered with silver nitrate (IC_{50} value; Figure 2(c); Table 2) compared to control cells for 72 h. However, early apoptotic cells increased 27.2-fold in cisplatin-treated cells (Figure 2(b); Table 2), and increased 9-fold in silver nitrate–treated cells for 72 h (Figure 2(c); Table 2).

The caspase-3 activity in A549 cells treated by silver nitrate

Caspase-3 is one of the cysteine proteases which plays a major role in the execution of apoptosis. Caspase-3 activity was measured by flow cytometry assay using caspase-3 antibody. The activation of caspase-3 was found to be increased in cells administered with cisplatin (IC_{50} value) compared with control cells (Figure 2(b)), but not for silver nitrate (IC_{50} value), after 72 h of incubation (Figure 2(c); Table 3).

The mitochondrial membrane potential in A549 cells treated by silver nitrate

Mitochondrial membrane potential ($\Delta\Psi m$), an important parameter of mitochondrial function, is often employed as an indicator of cellular viability. The lipophilic dye (JC-1) accumulates in the mitochondria to indicate the dissipation of $\Delta\Psi m$. The IC_{50} of cisplatin and silver nitrate caused a reduction in $\Delta\Psi m$ when administered for 72 h (Figure 2(b) and (c); Table 4). The IC_{50} of cisplatin reduced $\Delta\Psi m$ upto 5.4-fold compared to control cells, whereas the IC_{50} of silver nitrate decreased $\Delta\Psi m$ upto 1.4-fold compared to control cells (Table 4).

Immunocytochemical identification of silver nitrate–treated A549 cells

The presence of apoptosis was determined by hematoxylin and eosin (H&E), paraffin embedded TUNEL, BrdU, and Bcl-2 and Bax stainings using light microscopy (Figure 3). The apoptotic quantification was expressed as the percentage of staining multiplied by staining intensity. The scores quantification of the incidence of macroscopic was higher in treated cells than in control cells (Table 5). Based on the results of immunocytochemical staining (TUNEL, BrdU, and Bcl-2 and Bax), the IC_{50} values of cisplatin-induced apoptosis were compared to control cells (Figure 3(a) and (b); Table 5). Furthermore, the IC_{50} of silver nitrate–induced apoptosis at H&E, TUNEL, BrdU, and Bcl-2 and Bax staining were recorded (Figure 3(a) and (c); Table 5).

Table 1. The half-maximal inhibitory concentration (IC_{50}) values of silver nitrate and cisplatin for 24, 48, and 72 h.

Concentration (µM)	24 h	48 h	72 h
Cisplatin (IC_{50})	31.25 ± 1.76	5.1 ± 1.69	3 ± 0
Silver nitrate (IC_{50})	24.75 ± 0.35	15 ± 0	13.5 ± 2.12

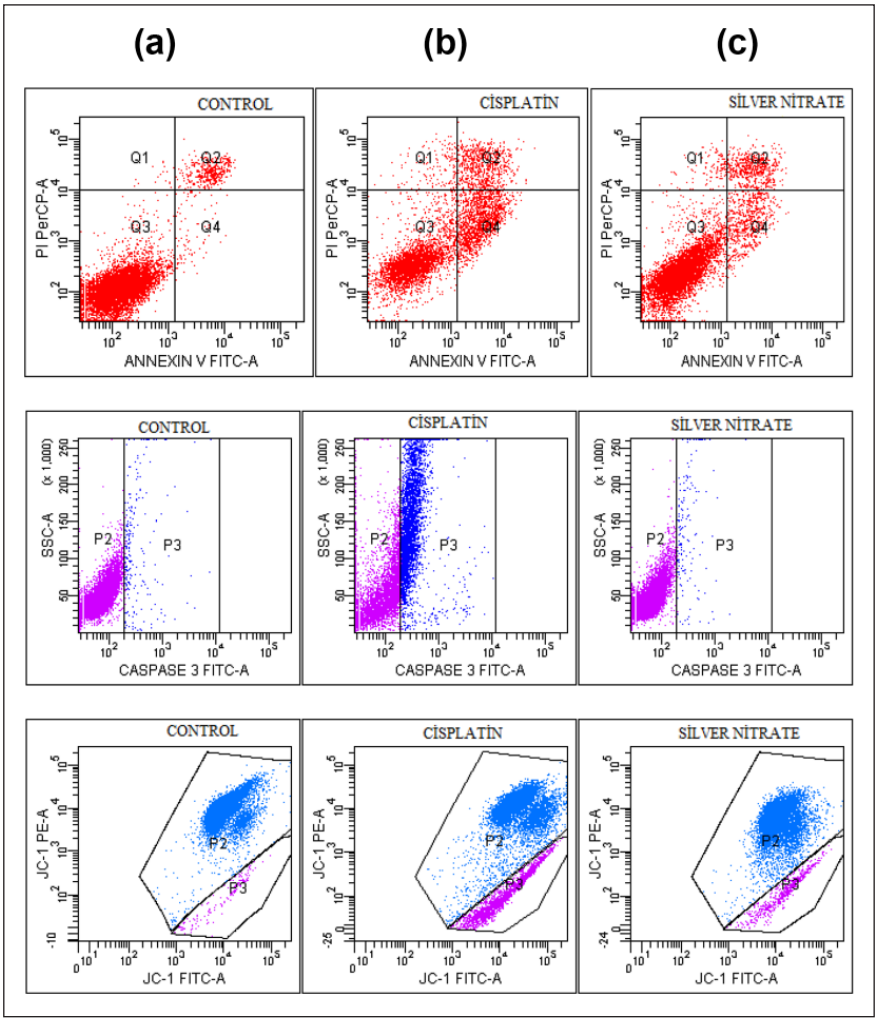

Figure 2. The effects of silver nitrate on apoptosis: the A549 cells were treated with silver nitrate and positive control cisplatin for 72 h. The flow cytometry analyses (Annexin V-FITC/PI, Caspase-3 and Mitochondrial membrane potential) were performed. At least, 10,000 cells were analyzed per sample and quadrant analysis was performed.

Table 2. The quantitative analysis of early and late apoptosis by flow cytometry. The percentages of early and late apoptotic cells were demonstrated in silver nitrate–treated cells.

Groups	Q1	Q2	Q3	Q4
Control (%)	0.2	4.1	94.8	0.9
Cisplatin (%)	2.6	11.5	61.5	24.5
Silver nitrate (%)	1.5	7.2	83.2	8.1

Q1: Necrosis; Q2: Late apoptosis; Q3: viability; Q4: Early apoptosis.

Confocal microscopy of silver nitrate–treated A549 cells

According to the microscopy results, the cells administered with cisplatin and silver nitrate were labeled by Annexin FITC (green) and acridine orange (red; Figure 4). We observed apoptotic features, such as intact nuclear morphology, nuclear fragmentation, condensed nucleus, ghost cell, and condensed chromosome on treated cells (Figure 4(b) and (c))

Transmission electron microscopy of silver nitrate–treated A549 cells

The A549 cells were exposed to IC_{50} dose of silver nitrate for 72 h. Transmission electron microscopy (TEM)

Table 3. The quantitative analysis of caspase-3 activity by flow cytometry. The percentages of caspase-3-activated cells were determined in silver nitrate–treated cells.

Groups	P2	P3
Control (%)	98.1	2.1
Cisplatin (%)	61.2	40.7
Silver nitrate (%)	98.6	1.5

P2: living cells; P3: caspase-3-activated cells.

Table 4. The quantitative analysis of mitochondrial membrane potential by flow cytometry: the percentages of mitochondrial membrane depolarized cells were detected in silver nitrate–treated cells.

Groups	P2	P3
Control (%)	95.3	4.1
Cisplatin (%)	76.6	22.3
Silver nitrate (%)	93.6	5.9

P2: mitochondrial membrane polarized cells; P3: mitochondrial membrane depolarized cells.

analyzed ultrastructural cell changes. The structural changes recorded all evidences of apoptotic activity, such as condensed nucleus and chromosome, and fragmented nuclei (Figure 4). The structural changes on cells caused by 72 h of exposure to the IC_{50} dose of silver nitrate were shown in Figure 4(b) (condensed nucleus and chromosome) and in Figure 4(c) (fragmented nuclei). In contrast, control cells had a normal cell ultrastructure.

Gene array analysis in A549 cells treated by silver nitrate

To evaluate the quality and consistency of silver nitrate, the scatterplot and correlation map with hierarchical clustering analyses were performed with microarray analysis. The upregulated and downregulated genes were found by microarray analysis (Figure 5; Table 6). The 16 upregulated genes and 10 downregulated genes showed apoptotic activity: *BAX*, *EI24*, *PEA15*, *CYFIP2*, *DKK1*, *TFPI2*, *ABCA1*, *FEZ1*, *CLDN1*, *IGFBP7*, *TP53INP1*, *FAS*, *TNFRSF10B*, *TP53I3*, *CDKN1A*, and *TNFSF14* genes were upregulated with cisplatin administration; *CCNB1*, *FGFR3*, *CDCA5*, *CCNB2*, *ASF1B*, *EIF2C2*, *FOXC1*, *ANG*, *ANG* and *NUCKS1* genes were downregulated with cisplatin administration (Figure 5; Table 7). However, *CCNY*, *HNRNPL*, *ASF1B*, *PIAS4*, *HNRNPH1*, *EIF2C2*, *TAF15*, *FOXC1*, *LEP*, and *PCB2* genes were downregulated with silver nitrate administration. *ASF1*, *EIF2C2*, and *FOXC1* genes were downregulated with the administration of the both agents. This indicates that silver nitrate may affect same genes targeted by cisplatin as well (Figure 5).

Discussion

Our aim was to investigate whole genome and apoptotic signaling pathways of silver nitrate in A549 adenocarcinomic human alveolar basal epithelial cells. Silver nitrate administered to A549 cells significantly induced cell death and showed inhibitory effects at low doses, inducing apoptotic signaling pathways. In this study, silver nitrate increased early/late apoptosis and depolarized mitochondrial membrane potential. The reduced mitochondrial membrane potential has been implicated in the signal pathways leading to apoptosis. In this study, early apoptosis, which is the main cause of cell death, was increased by silver nitrate compared to control cells.

The recent studies have demonstrated that silver compounds have in vitro anticancer activities. Silver nitrate has been administered in immortalized murine fibroblast cell line L929 and the inhibitory effects have been determined.[12,13] Park et al.[13] have showed that IC_{20} value of silver nitrate was detected as 7.1 µg/mL for L929 cells. Kaba and Egorova[14] suggested that silver nitrate was moderately cytotoxic toward U937 (human leukemic monocyte lymphoma) cell line at different concentrations. In another study, the different concentrations of silver nitrate (1, 10, 50, and 100 µg) have been tested in the growth of MDA-MB-231 cells, and the cell viability has been measured. Silver nitrate was administered at a concentration of 100 µg/mL of the cells.[15] Cisplatin and silver nitrate have also been administered against OVCAR-3 (ovarian), MB157 (breast), and Hela (cervical) human cancer cell lines for 72 h. The inhibitory effects of cisplatin have been determined at 12, 25, and 25 µM for 72 h and the inhibitory effects of silver nitrate (IC_{50} value) have been obtained at 35, 5, and 50 µM for 72 h. Silver nitrate has been observed to be most effective in the MB157 cell line compared to OVCAR-3 and Hela cell lines due to ultra low dose (5 µM) as IC_{50} value. Silver nitrate has no effect as cisplatin on OVCAR-3 and Hela cells but has significant effect on MB157 cells.[16] Our results show that IC_{50} values of silver nitrate and cisplatin are 13.5 and 3 µM, respectively, in A549 cells. This means that silver nitrate and cisplatin are more effective on A549 cells compared to Hela and OVCAR-3 cells. Miura and Shinohara[17] have demonstrated that silver nitrate has powerful inhibitor influences on Hela cell lines and triggered apoptosis causing the oxidative stress. IC_{50} was determined at 17 µg. The early/late apoptotic effects of silver nitrate have been observed in a dose-dependent manner. The late apoptotic cells have increased compared to early apoptotic cells.[17] Our findings showed that early apoptotic cells (Annexin V-positive, PI-negative) increased 5.2-fold compared to late apoptotic cells (Annexin V-positive, PI-positive). It is known that apoptotic cells are Annexin-V-positive and PI-negative. At the same time, Annexin V-positive and PI-positive cells

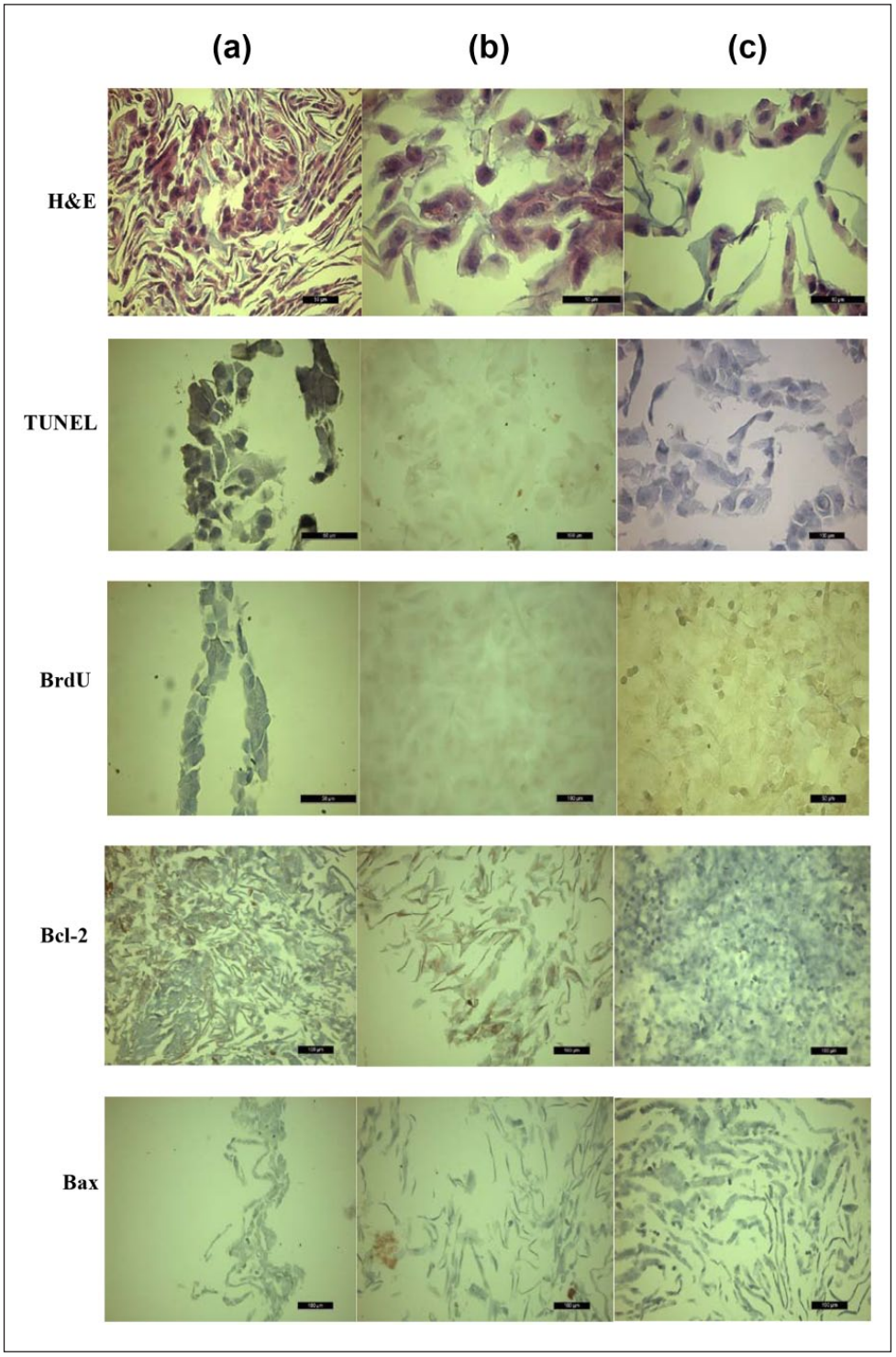

Figure 3. The assessment of apoptosis by immunocytochemical staining using light microscopy: (a) untreated cells; (b) A549 cells treated with IC_{50} value of cisplatin; and (c) A549 cells treated with IC_{50} value of silver nitrate.

are secondary necrotic cells.[18] Our results showed that there has been less necrosis in our study compared to the results of Miura and Shinohara.[17] The inhibition of A549 cells has been induced by silver nitrate. The lowest concentration effect of silver nitrate has been detected at 30 µM for 24 h.[19] In this study, the lowest concentration effect of silver nitrate has been found at 24.75 µM for 24 h.

Foldbjerg et al.[20] have revealed that silver ions induced apoptotic DNA damage by increasing the reactive oxygen species (ROS) levels in A549 cells. We demonstrated that

Table 5. The quantification of apoptosis scores by immunocytochemical staining.

Groups	Control	Cisplatin	Silver nitrate
H&E	2	2	3
TUNEL	0	3	1
BrdU	0	3	3
Bcl-2	3	1	0
Bax	0	1	0

H&E: hematoxylin and eosin; 3: maximum staining; 2: moderate staining; 1: less staining; 0: no staining.

silver nitrate induced apoptosis depending on depolarized mitochondrial membrane potential in A549 cells. Caspase-3 activity was not induced by silver nitrate. These findings indicate that silver nitrate triggers different apoptotic pathways in different cell lines.[20] In addition, HaCaT keratinocytes and K562 erythroleukemia mammalian cell lines have been exposed to various doses of silver nitrate and it has been effective at 6.4 and 3.5 µM. Administration of silver nitrate at low doses (<1 µM) induced chromatin changes in K562 cells. The nuclear changes, such as condensed chromatin, have been induced by silver nitrate. Silver nitrate concentrations (10–15 µM) caused nuclear shrinkage with an infrequent formation of apoptotic bodies.[21] In another study, fluorescent microscopic images have shown that silver nitrate has caused the formation of apoptotic bodies in MDA-MB-231 human breast cancer cells.[15] In our study, fragmented nuclei and condensed chromosome were observed in A549 cells by confocal and TEM images. According to immunocytochemical results (H&E, TUNEL, and BrdU), silver nitrate induced apoptosis. Miura and Shinohara[17] have indicated that upregulated *HO-1*, *MT-2A*, and *HSP-70* stress-response genes induced apoptosis by silver nitrate.[17] Our results indicated that downregulated *CCNY*, *HNRNPL*, *ASF1B*, *PIAS4*, *HNRNPH1*, *EIF2C2*, *TAF15*, *FOXC1*, *LEP*, and *PCB2* genes induced apoptosis by silver nitrate. *CCNY* gene expression is not known to be associated with human lung cancer. However, the overexpression of *CCNY* gene has been determined in non–small cell lung cancer (NSCLC) cells. The downregulated *CCNY* gene has inhibited lung cancer growth.[22] Goehe et al.[23] have suggested that downregulated *HNRNPL* triggered the loss of tumorigenic capacity by increasing caspase-9 activity in NSCLC.[23] In another study, overexpression of *ASF1B* has been observed in breast cancer. The downregulated *ASF1B* may be an important target for cancer treatment.[24] In NCSLC of H1299 cell line, *PIAS4* gene expression suppressed p53 and Bax genes. The inhibition of *PIAS4* activity is seen as a new therapeutic application.[25] The downregulated *TAF15* has been identified as an inhibitor of cell proliferation and caused apoptosis.[26] The overexpression of leptin (*LEP*) induced cell proliferation in hepatocellular liver cancer (HepG2) cells.[27] The overexpression of *PCBP2* leads to

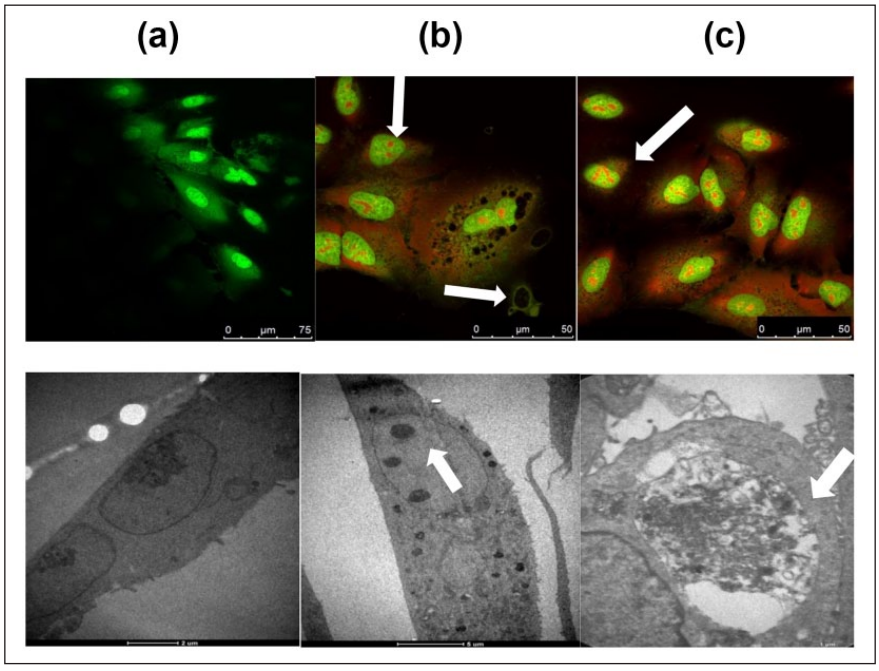

Figure 4. Confocal microscopy and TEM visualizations of A549 cells using Annexin FITC and acridine orange dyes: (a) untreated cells (40× and 8200×); (b) treated cells with IC_{50} dose of cisplatin for 72 h (40× and 4200×); and (c) treated cells with IC_{50} dose of silver nitrate for 72 h (40× and 16,500×). The arrows show apoptotic bodies.

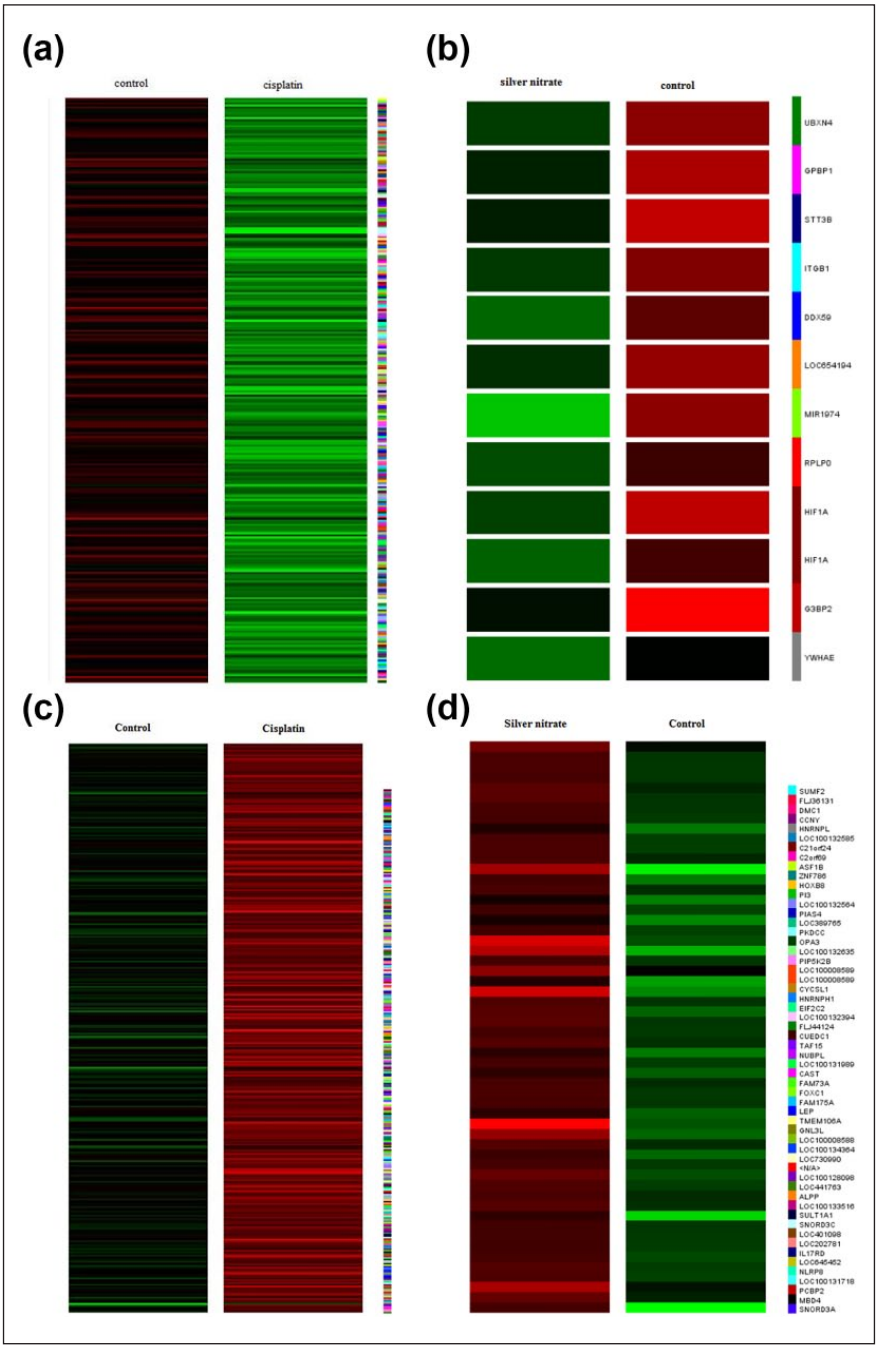

Figure 5. The expression profiling displayed by whole genome microarray analysis (red: downregulated, green: upregulated): (a–b) the upregulated genes treated with cisplatin and silver nitrate compared to control cells; (c–d) the downregulated genes treated with cisplatin and silver nitrate compared to control cells. Technical replicate analysis was performed. Raw microarray data have been converted to electronic data by GenomeStudio program.

Table 6. The statistics of upregulated and downregulated genes were analyzed by microarray assay.

Genes	Cisplatin	Silver nitrate
Upregulated	280	12
Downregulated	364	56

production of oncogenic protein in human gastric cancer.[28] *PCBP2* has been downregulated in glioma cell lines (T98G, U87MG, A172, U251, and CCF-STG1) and has been shown as a target in the treatment of cancer.[29] However, upregulation of *BAX*, *EI24*, *PEA15*, *CYFIP2*, *DKK1*, *TFPI2*, *ABCA1*, *FEZ1*, *CLDN1*, *IGFBP7*, *TP53INP1*, *FAS*, *TNFRSF10B*, *TP53I3*, *CDKN1A*, and

Table 7. Apoptosis-related genes regulated by cisplatin and silver nitrate in A549 cells.

Gene symbols		
Cisplatin		Silver nitrate
Upregulated	Downregulated	Downregulated
BAX	*CCNB1*	*CCNY*
EI24	*FGFR3*	*HNRNPL*
PEA15	*CDCA5*	*ASF1B*
CYFIP2	*CCNB2*	*PIAS4*
DKK1	*ASF1B*	*HNRNPH1*
TFPI2	*EIF2C2*	*EIF2C2*
ABCA1	*FOXC1*	*TAF15*
FEZ1	*ANG*	*FOXC1*
CLDN1	*ANG*	*LEP*
IGFBP7	*NUCKS1*	*PCB2*
TP53INP1		
FAS		
TNFRSF10B		
TP53I3		
CDKN1A		
TNFSF14		

TNFSF14 genes and downregulation of *CCNB1*, *FGFR3*, *CDCA5*, *CCNB2*, *ASF1B*, *EIF2C2*, *FOXC1*, *ANG*, and *NUCKS1* genes caused by cisplatin indicated apoptotic signaling pathways. *ASF1*, *EIF2C2*, and *FOXC1* genes were downregulated by both silver nitrate and cisplatin. This indicates that silver nitrate may affect same genes targeted by cisplatin as well. According to immunocytochemical and microarray results, silver nitrate has no effects on Bcl-2 and Bax expression levels. Furthermore, according to caspase-3 analysis result, silver nitrate had no effect on caspase-3 activity. The absence of caspase-3 activity was also confirmed by whole genome expression microarray analysis. This suggests that apoptosis may be affected by a caspase-independent pathway (apoptosis inducing factor (AIF) and cadherins, etc). This result may be a subject for future research.

In conclusion, we studied gene analyses and apoptotic effects of silver nitrate in A549 cells. Our findings revealed that the proportion of apoptotic cells was increased by the administering A549 cells with silver nitrate. These results indicate that silver nitrate may be a pharmaceutical inhibitor against lung cancers.

Acknowledgements

This article does not include any studies with human participants or animals.

Declaration of conflicting interests

The author(s) declared no potential conflicts of interest with respect to the research, authorship, and/or publication of this article.

Funding

This work was supported by Anadolu University, Scientific Research Project (no. 1305F088).

References

1. Stewart BW and Kleihues P. *World cancer report*. Geneva: International Agency for Research on Cancer (IARC), World Health Organization (WHO), 2003, pp. 182–185.
2. Hou Z-B, Lu K-J, Wu X-L, et al. In vitro and in vivo antitumor evaluation of berbamine for lung cancer treatment. *Asian Pac J Cancer Prev* 2014; 15(4): 1767–1769.
3. Sihoe ADL and Yim APC. Lung cancer staging. *J Surg Res* 2004; 117: 92–106.
4. Beadsmoore CJ and Screaton NJ. Classification, staging and prognosis of lung cancer. *Eur J Radiol* 2003; 45: 8–17.
5. Giard DJ, Aaronson SA, Todaro GJ, et al. In vitro cultivation of human tumors: establishment of cell lines derived from a series of solid tumors. *J Natl Cancer Inst* 1973; 51(5): 1417–1423.
6. Arora S, Jain J, Rajwade JM, et al. Cellular responses induced by silver nanoparticles: in vitro studies. *Toxicol Lett* 2008; 179: 93–100.
7. Foldbjerg R, Olesena P, Hougaard M, et al. PVP-coated silver nanoparticles and silver ions induce reactive oxygen species, apoptosis and necrosis in THP-1 monocytes. *Toxicol Lett* 2009; 190: 156–162.
8. Siciliano TJ, Deblock MC, Hindi KM, et al. Synthesis and anticancer properties of gold(I) and silver(I) N-heterocyclic carbene complexes. *J Organomet Chem* 2011; 696: 1066–1071.
9. U.S. Environmental Protection Agency. *Integrated risk information system (IRIS)*. Cincinnati, OH: Environmental Criteria and Assessment Office of Environmental Assessment, 1992.
10. Reed JC. Dysregulation of apoptosis in cancer. *J Clin Oncol* 1999; 17(9): 2941–2953.
11. Ghobrial IM, Witzig TE and Adjei AA. Targeting apoptosis pathways in cancer therapy. *CA Cancer J Clin* 2005; 55: 178–194.
12. Müller G and Kramer A. Biocompatibility index of antiseptic agents by parallel assessment of antimicrobial activity and cellular cytotoxicity. *J Antimicrob Chemoth* 2008; 61: 1281–1287.
13. Park MVDZ, Neigh AM, Vermeulen JP, et al. The effect of particle size on the cytotoxicity, inflammation, developmental toxicity and genotoxicity of silver nanoparticles. *Biomaterials* 2011; 32: 9810–9817.
14. Kaba SI and Egorova EM. In vitro studies of the toxic effects of silver nanoparticles on HeLa and U937 cells. *Nanotechnol Sci Appl* 2015; 8: 19–29.
15. Krishnaraj C, Muthukumaran P, Ramachandran R, et al. Acalypha indica Linn: biogenic synthesis of silver and gold nanoparticles and their cytotoxic effects against MDA-MB-231, human breast cancer cells. *Biotechnol Rep* 2014; 4: 42–49.
16. Medvetz DA, Hindi KM, Panzner MJ, et al. Anticancer activity of Ag(I) n-heterocyclic carbene complexes derived from 4,5-dichloro-1h-imidazole. *Met Based Drugs* 2008; 2008: 384010.
17. Miura N and Shinohara Y. Cytotoxic effect and apoptosis induction by silver nanoparticles in HeLa cells. *Biochem Biophys Res Commun* 2009; 390: 733–737.

18. Brauchle E, Thude S, Brucker SY, et al. Cell death stages in single apoptotic and necrotic cells monitored by Raman microspectroscopy. *Sci Rep* 2014; 4: 4698.
19. Koch M, Kiefer S, Cavelius C, et al. Use of a silver ion selective electrode to assess mechanisms responsible for biological effects of silver nanoparticles. *J Nanopart Res* 2012; 14: 646.
20. Foldbjerg R, Dang DA and Autrup H. Cytotoxicity and genotoxicity of silver nanoparticles in the human lung cancer cell line, A549. *Arch Toxicol* 2011; 85: 743–750.
21. Nagy G, Turani M, Kovacs KE, et al. Chromatin changes upon silver nitrate treatment in human keratinocyte HaCaT and K562 erythroleukemia cells. In: G Banfalvi (ed.) *Cellular effects of heavy metals*. London: Springer, 2011, pp. 195–217.
22. Yue WT, Zhao XT, Zhang L, et al. Overexpression of cyclin Y in non-small cell lung cancer is associated with cancer cell proliferation. *Sci China Life Sci* 2010; 53(4): 511–516.
23. Goehe RW, Shultz JC, Murudkar C, et al. hnRNP L regulates the tumorigenic capacity of lung cancer xenografts in mice via caspase-9 pre-mRNA processing. *J Clin Invest* 2010; 120(11): 3923–3939.
24. Corpet A, De Koning L, Toedling J, et al. Asf1b, the necessary Asf1 isoform for proliferation, is predictive of outcome in breast cancer. *EMBO J* 2011; 30: 480–493.
25. Chien W, Lee KL, Ding LW, et al. PIAS4 is an activator of hypoxia signalling via VHL suppression during growth of pancreatic cancer cells. *Br J Cancer* 2013; 109: 1795–1804.
26. Ballarino M, Jobert L, Dembélé D, et al. TAF15 is important for cellular proliferation and regulates the expression of a subset of cell cycle genes through miRNAs. *Oncogene* 2013; 32(39): 4646–4655.
27. Chen C, Chang Y-C, Liu C-L, et al. Leptin induces proliferation and anti-apoptosis in human hepatocarcinoma cells by up-regulating cyclin D1 and down-regulating Bax via a Janus kinase 2-linked pathway. *Endocr Relat Cancer* 2007; 14: 513–529.
28. Hu C-E, Liu Y-C, Zhang H-D, et al. The RNA-binding protein PCBP2 facilitates gastric carcinoma growth by targeting miR-34a. *Biochem Biophys Res Commun* 2014; 448: 437–442.
29. Chen X, Hao B, Liu Y, et al. The histone deacetylase SIRT6 suppresses the expression of the RNA-binding protein PCBP2 in glioma. *Biochem Biophys Res Commun* 2014; 446: 364–369.